KSÜ Mühendislik Bilimleri Dergisi, 27(4), 2024
Araştırma Makalesi

KSU J Eng Sci, 27(4), 2024
Research Article

Kahramanmaras Sutcu Imam University
Journal of Engineering Sciences

Geliş Tarihi : 27.03.2024
Kabul Tarihi : 13.07.2024

Received Date : 27.03.2024
Accepted Date : 13.07.2024

# THE EFFECTS OF THE EARTHQUAKE INCIDENT ANGLE ON AN RC BUILDING

## DEPREM YÖNLENDİRME AÇISININ BETONARME BİR BİNA ÜZERİNDE ETKİLERİ

*Soukaina MELLOUK* [1] (ORCID: 0000-0002-2211-3722)
*Ebru HARMANDAR*[2*] (ORCID: 0000-0001-9802-2993)

[1] Muğla Sıtkı Koçman Üniversitesi, İnşaat Mühendisliği Bölümü, Muğla, Türkiye

* Sorumlu Yazar / Corresponding Author: Soukaina MELLOUK

**ABSTRACT**

Current building codes necessitate the inclusion of two ground motion acceleration components in the dynamic analysis of structures. However, researches indicate that the orientation of the chosen ground motion data can significantly impact the structural response. This study investigates the influence of the incident angle on a 10-story reinforced concrete building, considering different earthquake selection criteria. Specifically, it is aimed to identify the direction of the seismic data that yields the largest peak ground acceleration by applying rotations with specific angles. Subsequently, the dynamic analysis is performed using both the original and the rotated records that produce the highest acceleration. To ensure a comprehensive evaluation, the earthquake data is classified based on soil types, fault mechanisms, and Aria's intensity. The results of the dynamic analyses for both the original and oriented data sets are compared, focusing on parameters such as roof displacement, base shear, acceleration and displacement time histories, and acceleration and displacement spectra. Our findings reveal that the base shear and roof displacement obtained from the rotated earthquake data generally exceed those obtained from the original data. This underscores the importance of considering the influence of ground motion direction in structural analysis and design.

**Keywords:** Incident angle, reinforced concrete structure, time history analysis, soil types, near/far field effect

**ÖZET**

Mevcut bina mevzuatı, yapıların dinamik analizine iki yer hareketi ivme bileşeninin dahil edilmesini gerektirmektedir. Ancak araştırmalar, seçilen yer hareketi verilerinin yönünün yapısal davranışı önemli ölçüde etkileyebileceğini göstermektedir. Bu çalışma, sismik yer hareketinin yönlendirme açısının 10 katlı betonarme bir bina üzerindeki etkisini farklı deprem seçim kriterlerini dikkate alarak araştırmaktadır. Spesifik olarak, belirli açılarla rotasyonlar uygulayarak en büyük yer ivmesini sağlayan sismik verilerin yönünü belirleme hedeflendi. Daha sonra, hem orijinal deprem kayıtlarını hem de en yüksek ivmenin elde edildiği döndürülmüş deprem kayıtları kullanılarak dinamik analizler gerçekleştirildi. Kapsamlı bir değerlendirme yapmak için deprem verileri zemin sınıflarına, fay mekanizmalarına ve Arias şiddetine göre sınıflandırdı. Dinamik analizden elde edilen sonuçlar; çatı deplasmanı, taban kayması, ivme-yer değiştirme verileri ve ivme-yer değiştirme spektrumları göz önünde bulundurularak her iki durumdaki deprem kayıtları için karşılaştırma yapıldı. Bulgularımız, döndürülmüş deprem verilerinden elde edilen taban kesme ve çatı deplasmanlarının genellikle orijinal verilerden elde edilen değerleri aştığını ortaya koymaktadır. Bu, yapısal analiz ve tasarımda yer hareketi yönünün etkisinin dikkate alınmasının önemini vurgulamaktadır.

**Anahtar Kelimeler:** Yönlendirme açısı, betonarme yapılar, zaman tanım alanında analiz, zemin tipleri, yakın/uzak fay etkisi

ToCite: MELLOUK, S., & HARMANDAR, E., (2024). The Effects of the Earthquake Incident Angle on an RC Building. *Kahramanmaraş Sütçü İmam Üniversitesi Mühendislik Bilimleri Dergisi*, 27(4), 1197-1211.

## INTRODUCTION

The creation of pressure resulting from tectonic plate movement well-known earthquakes results from the pressure created by tectonic plate movement, the instant release of this energy is transmitted as seismic waves captured by seismometers. In civil engineering, seismic data is crucial for performing time history analysis on structures to assess their response during an earthquake. Seismic data might be recorded in the east-west and north-south directions or at various angles depending on the location of the seismometer which gives another complexity because of the unknown direction in which can an earthquake hit the structure.

The effect of the orientation of seismic ground motion on structures is very important for the design of structures. Meanwhile, this will help the structural engineers to improve the design of the building and construct a more resistant building against earthquakes. Many researchers have studied the effect of the propagation of earthquake ground motion data.

Sun et al. (2016) introduced a novel approach to analyse the impact of ground motion direction on structures. Their method involves rotating earthquake data by specific angles (θ). Remarkably, they discovered that varying θ significantly affects the spectral values, peak points, and even the predominant period of the data. They demonstrated that identifying the θ angle that leads to the most significant change in ground motion can provide valuable insights into potential failure mechanisms of structures. This information, in turn, can be leveraged to enhance structural design and resilience against earthquakes. In contrast to Sun et al. (2016), Kostinakis et al. (2012) considered a different approach. They analyzed a three-story building subjected to a horizontal seismic component while systematically rotating it through various angles (θ). They aim to assess how the orientation of the ground motion (represented by θ) affects the response of the reinforced concrete structure. They proposed that, indeed, the analysis of such structures is significantly influenced by the angle of seismic shaking.

Altunışık & Kalkan (2017) suggested the response of a 5-story building under the 1994 Erzincan earthquake in nineteen directions (0 to 90 degrees). These analyses show that the response of the building is influenced by the angle of seismic input motion. For instance, the maximum differences between the X and Y directions range from 54.54% and 37.15%. Additionally, both the axial force and bending moment can exceed the normal cases of 44 %, summarizing the change of angles. This can lead to an increase in the displacements and internal forces which means that there is no specific angle that can give the maximum value. Also, the far-field and near-field effects play an important role in finding the maximum value. Ruiz-Garcia & Negrete-Manriquez (2011) examined an existing steel frame building under a mainshock and aftershock seismic sequences on a far-field and near-fault of the 1994 Northridge and 1980 Mammoth earthquakes. The investigation of the ground motion direction and duration based on 3117 horizontal motions from the PEER database has been studied by Lee (2014). They considered the relation between strong-motion duration, orientation, the magnitude of the earthquake, and the relation between the distance of source and site, by obtaining the orientations at 0, 50, and 100 percentiles.

Hong et al. (2009) provided the earthquake ground motion data in the horizontal plane, encompassing bidirectional horizontal ground motions, for both Mexican interplate and in-slab earthquake data. Extensive statistical analyses of PSA (Pseudo-Spectral Acceleration) are conducted for the assessment. The ratio of the PSA to the maximum resulting PSA is calculated as done with California data. This ratio is independent from the maximum earthquake magnitude, the focal depth, the earthquake distance, and the resulting PSA. Collections of response ratios and ground motion prediction equations are applicable for the bidirectional horizontal ground motion data for Mexican interplate and in-slab earthquakes. The analytical formula was developed by Athanatopoulou (2005) for the determination of the critical angle of seismic incidence and the consistent maximum value of a response parameter of structures with three components: two horizontal components applied along with arbitrary directions and a vertical component of earthquake ground motion. Huang et al. (2009) studied one hundred forty-seven pairs of ground motion records of the moment magnitude ($M_W$) greater than 6.5 and the closest distance from the site to the fault rupture plane ($R_{rup}$) smaller than 15 km. They analyzed to examine the alignment of maximum spectral demand in the near-fault region. The analyses were carried out across four-period ranges, clearly indicating that there is characteristically an axis where the spectral demands closely align or are equal to the maximum demands. Kostinakis et al., (2018) provided that the incident angle of the ground motion significantly impacts the seismic performance and the damage level of the structures, even when their plan view is double-symmetric and relatively straightforward. The degree to which the orientation of the seismic data influences the damage response depends on the building and the distance between the record and the fault rupture. Generally, near-fault ground motions lead to a deteriorated damage state of the

structures compared to that resulting from the utilization of far-fault records as seismic input. Ghazizadeh et al. (2013) investigated building design affected by the direction of the earthquake they noticed that the scaling factor used to account for earthquake direction doesn't change that much between different building designs. Nevertheless, the methods used to evaluate building performance and the earthquake data itself can influence the importance of directionality. Pinzon et al. (2021) investigated the response of the structures affected instantly by the direction of the Earthquake. So, this research indicates that a building response can highly change according to the angle of the earthquake waves that is proportional to its orientation, that's why containing directionality in a structural analysis is fundamental. It ameliorates the evaluation of potential earthquake damage, especially for critical structures like hospitals, schools, nuclear plants, and other facilities, cause these facilities need to carry on functional after an earthquake to ensure public safety and recovery efforts, On the other hand, Cantagallo et al (2024) examined many recent studies (up to February 2024) on how earthquakes affect buildings and still, there's no way to account for direction yet, cause earthquakes can hit from any direction, also not all directions put the same amount of stress on a building. Normally engineers often make assumptions about earthquake direction, which could underestimate the strain that the building could have. This review suggests that future codes could be improved by giving engineers clear instructions on how to account for shaking direction and teaching them how to analyse buildings for multiple earthquake scenarios. However, Bugueño et al. (2021) tested how earthquake direction affects buildings using computer models of different designs (shear walls, frames, combinations). They didn't realize the worst shaking direction, instead, the different directions of stiffness building are very important. Hence, the shaking earthquake can cause more cracks or displacement in a building's weaker direction, but combining materials seems to make buildings less sensitive to direction, and frame-only buildings might be a safe design approach based on initial tests. The study has limitations cause the used models didn't examine other details like building height, number of stories, or the intensity of the earthquake zone that's why they suggest more research using real buildings to get more information on how earthquake direction affects building response.

Due to the uncertainty regarding the epicenter location of the subsequent earthquake, the seismic data should be applicable in any direction relative to the structure under analysis. Considering the relative disparities in the incident angles of consecutive earthquakes can notably impact the resulting seismic responses, as evidenced by the findings. As aforementioned, numerous researchers have investigated how the incident angle influences the performance of structures with a single earthquake scenario. In this study, one regular building is modelled and investigated. The building is subjected to ground accelerations with different criteria. The aim here is to observe the effect of earthquake data on the building in terms of earthquake orientation with different characteristics.

In this study, a 10-story reinforced concrete building is analysed using linear time history analysis by rotating the direction of the earthquake records. Earthquake data is selected considering the effect of the near and far field; site classes (soft, stiff, rock), and fault mechanisms (normal, reverse, strike-slip).

Earthquake records are rotated at intervals of 10°, and the incident angle at which the record has the highest acceleration value will be used in time history analysis. The original earthquake records and the earthquake records in the direction giving the highest acceleration are compared as a result of dynamic analysis.

Moreover, it is aimed to examine the effect of near and far field effects, compare the effect of soil classes, to investigate the structure behaviour while considering the fault mechanism; to observe the effect of high and low Arias intensities of ground motion recordings on the structure in terms of orientation.

## STRUCTURAL MODEL

The ten-story reinforced concrete (RC) structural model is designed with SAP2000 software, adhering to the specifications outlined in the Turkish Building Earthquake Code (TBEC, 2018). The model is designed as a frame system. The building stands 35m tall and features concrete with a compressive strength of 35 MPa. Steel reinforcement boasts a yield strength of 420 MPa. Beams have dimensions of 60cm x 70cm, while columns are modelled as 75cm x 60cm sections. The frame consists of five bays spaced 8m apart. The configuration of the building is represented in Figure 1 with a total weight of 337,572 kN and a fundamental period of 1.76 seconds.

## GROUND MOTION DATABASE

The earthquake ground motion data are selected from the PEER database according to the criteria shown in Table 1-Table 3. Earthquake data if needed are processed to remove the noise by using baseline correction, tapering, and

filtering. This research aims to explore the influence of the angles (between 0 and 90 degrees) on structural response. To achieve this, various earthquake data sets encompassing different characteristics are considered. The data are carefully organized based on the key criteria: near-field (with pulse) and far-field recordings, site classes (soft, stiff, rock), and fault mechanisms (normal, reverse, strike-slip). In this study, the issue isn't compared based on region. Instead, the incident angle is assessed in terms of the earthquake. Therefore, the scaling isn't conducted.

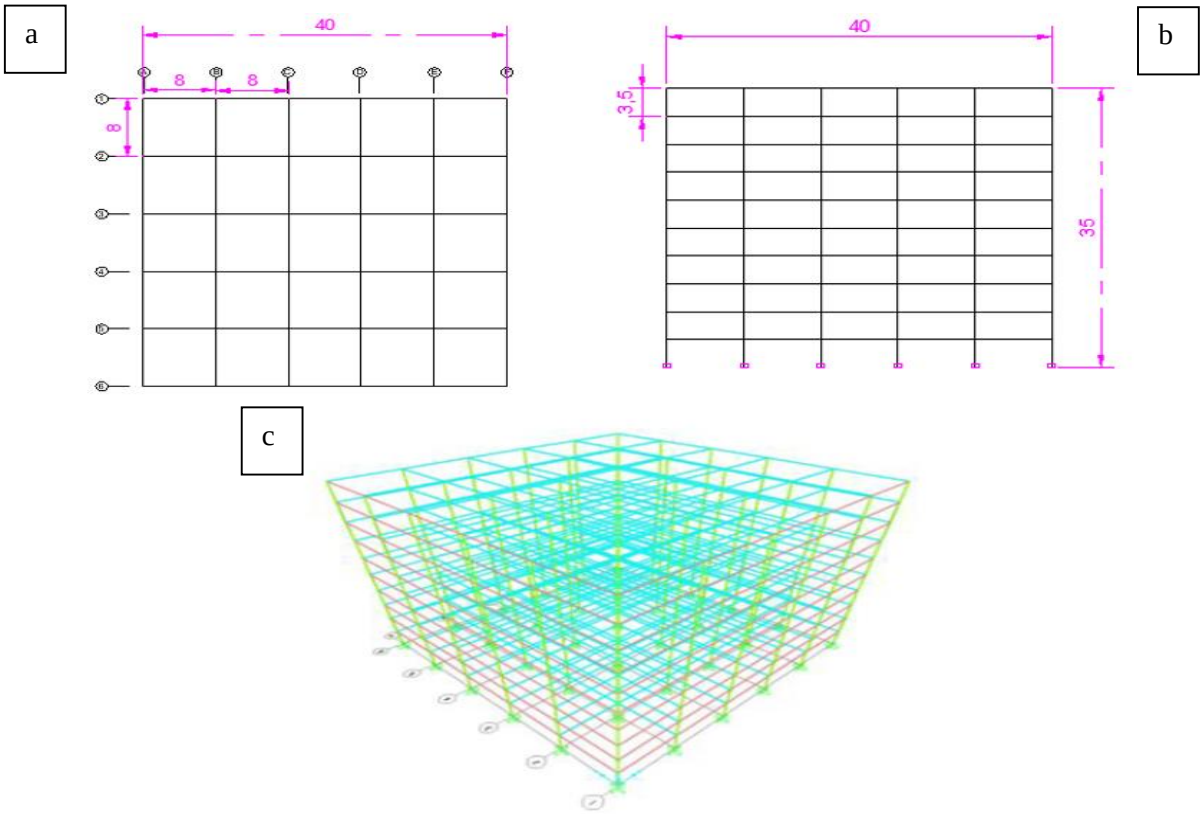


**Figure 1. a.** Plan View, **b.** Front View, **c.** Finite Element Model of the RC Building (the units are in m)

**Table 1.** General Properties of Earthquakes with Normal Fault Mechanism

| | | | | Earthquake Name | Record Sequence Number | $V_{s30}$ (m/s) | $R_{jb}$ (km) | Year | Station Name | Moment magnitude ($M_W$) | Arias Intensity (m/s) |
|---|---|---|---|---|---|---|---|---|---|---|---|
| NORMAL FAULT | Near Field (0-10 km) | Soft soil 0-400 m/s | Low Arias Intensity | Ancona-10, Italy | 4262 | 256.0 | 2.94 | 1972 | Ancona-Palombina | 4.3 | 0.1 |
| | | | Medium Arias Intensity | Kalamata, Greece | 564 | 382.21 | 6.45 | 1986 | Kalamata (bsmt) | 6.2 | 0.7 |
| | | | High Arias Intensity | Dinar, Turkey | 1141 | 219.75 | 0.0 | 1995 | Dinar | 6.4 | 2.0 |
| | | Stiff soil 400-760 m/s | Low Arias Intensity | Oroville-03 | 113 | 634.85 | 0.0 | 1975 | DWR Garage | 4.7 | 0.1 |
| | | | Medium Arias Intensity | Irpinia, Italy | 300 | 455.93 | 8.81 | 1980 | Calitri | 6.2 | 0.5 |
| | | | High Arias Intensity | L'Aquila, Italy | 4480 | 475.0 | 0.0 | 2009 | L'Aquila - V. Aterno - Centro Valle | 6.3 | 2.8 |
| | | Rock 760-1500 m/s | Low Arias Intensity | China Lake | 12675 | 1464.0 | 6.47 | 2007 | China Lake | 4.34 | 0.0 |
| | Far Field (50-100 km) | Soft soil 0-400 m/s | High Arias Intensity | Kozani, Greece | 1127 | 282.27 | 74.06 | 1995 | Larisa | 6.4 | 0.1 |
| | | Stiff soil 400-760 m/s | Low Arias Intensity | Little Skull Mtn, NV | 1745 | 515.4 | 99.44 | 1992 | Station #6-Las Vegas Calico Basin | 5.65 | 0.0 |
| | | | Medium Arias Intensity | Irpinia, Italy | 293 | 593.35 | 59.63 | 1980 | Torre Del Greco | 6.9 | 0.1 |
| | | | High Arias Intensity | Pelekanada, Greece | 484 | 527.96 | 154.5 | 1984 | Pelekanada | 5.0 | 0.2 |

**Table 2.** General Properties of Earthquakes with Reverse Fault Mechanism

| | | | | Earthquake Name | Record Sequence Number | $V_{s30}$ (m/s) | $R_{jb}$ (km) | Year | Station Name | Moment magnitude ($M_W$) | Arias Intensity (m/s) |
|---|---|---|---|---|---|---|---|---|---|---|---|
| REVERSE FAULT | Near Field (0-10 km) | Soft soil 0-400 m/s | Low Arias Intensity | Northridge | 1737 | 370.52 | 6.79 | 1994 | Sylmar - Converter Sta East | 5.28 | 0.2 |
| | | | Medium Arias Intensity | Niigata, Japan | 4210 | 331.63 | 7.45 | 2004 | NIG020 | 6.63 | 3.5 |
| | | | High Arias Intensity | Chi-Chi, Taiwan | 1513 | 363.99 | 0.0 | 1999 | TCU079 | 7.62 | 7.7 |
| | | Stiff soil 400-760 m/s | Low Arias Intensity | Coalinga | 410 | 458.09 | 7.92 | 1983 | Palmer Ave | 5.77 | 0.6 |
| | | | Medium Arias Intensity | Cape Mendocino | 828 | 422.17 | 0.0 | 1992 | Petrolia | 7.01 | 3.8 |
| | | | High Arias Intensity | Chi-Chi, Taiwan | 1507 | 624.85 | 0.0 | 1999 | TCU071 | 7.62 | 9.5 |
| | | Rock 760-1500 m/s | Low Arias Intensity | Loma Prieta | 765 | 1428.1 | 8.84 | 1989 | Gilroy Array | 6.93 | 1.7 |
| | | | Medium Arias Intensity | Loma Prieta | 3548 | 1070.3 | 3.22 | 1989 | Los Gatos - Lexington Dam | 6.93 | 1.9 |
| | | | High Arias Intensity | Tabas, Iran | 143 | 766.77 | 1.79 | 1978 | Tabas | 7.35 | 11.8 |
| | Far Field (50-100 km) | Soft soil 0-400 m/s | Low Arias Intensity | Taiwan SMART | 510 | 314.33 | 56.71 | 1986 | SMART1 | 6.32 | 0.2 |
| | | | Medium Arias Intensity | Loma Prieta | 784 | 306.3 | 72.09 | 1989 | Oakland - Title & Trust | 6.93 | 0.7 |
| | | | High Arias Intensity | Taiwan SMART | 578 | 285.09 | 57.13 | 1986 | SMART1 | 7.3 | 1.4 |
| | | Stiff soil 400-760 m/s | Low Arias Intensity | Georgia, USSR | 820 | 432.58 | 51.33 | 1991 | Zem | 6.2 | 0.1 |
| | | | Medium Arias Intensity | Kern County | 14 | 514.99 | 81.3 | 1952 | Santa Barbara Courthouse | 7.36 | 0.3 |
| | | | High Arias Intensity | Loma Prieta | 771 | 584.17 | 79.71 | 1989 | Golden Gate Bridge | 6.93 | 0.5 |
| | | Rock 760-1500 m/s | Low Arias Intensity | Chi-Chi, Taiwan | 2989 | 804.36 | 69.76 | 1999 | CHY102 | 6.2 | 0.1 |
| | | | Medium Arias Intensity | Iwate, Japan | 5650 | 891.55 | 64.27 | 2008 | IWTH18 | 6.9 | 0.4 |
| | | | High Arias Intensity | Iwate, Japan | 5646 | 816.31 | 99.04 | 2008 | IWTH14 | 6.9 | 0.9 |

## *Orientation of Strong Ground Motion Data*

While earthquake ground motion is recorded in three directions (X, Y, and Z), this study focuses specifically on the horizontal components (X and Y). We aim to investigate the impact of the strongest shaking direction on structures. Instead of analysing the entire waveform in each direction, the maximum peak ground acceleration (PGA) at any angle for each horizontal component is identified. This enables us to determine the direction that would generate the most intense shaking at a specific point and to identify the angle at which the earthquake causes the largest ground displacement and acceleration.

The structure is analysed using all available earthquake data to obtain time histories for base shear, roof displacement, acceleration, as well as displacement and acceleration response spectra. The second part focuses on the original X and Y components of a single earthquake. However, the station recording the data may be positioned at any angle, meaning the maximum peak ground motion might occur at an angle different from the X or Y axes (Figure 2).

The purpose is to rotate the data with angles differing from $\theta = 0°$ to $\theta = 90°$ based on Equation. (1) and Equation (2):

$$E'_X = E_X \cos(\theta) + E_Y \sin(\theta) \quad (1)$$

$$E'_Y = -E_X \sin(\theta) + E_Y \cos(\theta) \quad (2)$$

Following the calculation of earthquake data rotation along the X and Y axes at a specified angle ($\theta$) where peak ground acceleration is elevated, subsequent linear time history analysis is conducted. Base shear, roof displacement, acceleration, and displacement time histories are derived from the rotated earthquake data.

**Table 3.** General Properties of Earthquakes with Strike-slip Fault Mechanism

| | | | | Earthquake Name | Record Sequence Number | $V_{s30}$ (m/s) | $R_{jb}$ (km) | Year | Station Name | Moment magnitude ($M_W$) | Arias Intensity (m/s) |
|---|---|---|---|---|---|---|---|---|---|---|---|
| STRIKE-SLIP FAULT | Near Field (0-10 km) | Soft soil 0-400 m/s | Low Arias Intensity | Duzce, Turkey | 1615 | 338.0 | 9.14 | 1999 | Lamont 1062 | 7.14 | 1.0 |
| | | | Medium Arias Intensity | Duzce, Turkey | 1605 | 281.86 | 0.0 | 1999 | Duzce | 7.14 | 2.9 |
| | | | High Arias Intensity | Tottori, Japan | 3968 | 310.21 | 0.83 | 2000 | TTRH02 | 6.61 | 11.8 |
| | | Stiff soil 400-760 m/s | Low Arias Intensity | Duzce, Turkey | 1618 | 638.39 | 8.03 | 1999 | Lamont 531 | 7.14 | 0.4 |
| | | | Medium Arias Intensity | Big Bear | 901 | 430.36 | 7.31 | 1992 | Big Bear Lake - Civic Center | 6.46 | 3.3 |
| | | | High Arias Intensity | Duzce, Turkey | 1617 | 454.2 | 3.93 | 1999 | Lamont 375 | 7.14 | 10.0 |
| | | Rock 760-1500 m/s | Low Arias Intensity | Parkfield | 4083 | 906.96 | 4.66 | 2004 | Parkfield Turkey Flat | 6.0 | 0.2 |
| | | | Medium Arias Intensity | Kocaeli, Turkey | 1165 | 811.0 | 3.62 | 1999 | Izmit | 7.51 | 0.8 |
| | | | High Arias Intensity | Landers | 879 | 1369.0 | 2.19 | 1992 | Lucerne | 7.28 | 7.0 |
| | Far Field (50-100 km) | Soft soil 0-400 m/s | Low Arias Intensity | Hector Mine | 1812 | 387.12 | 84.87 | 1999 | Mill Creek Ranger Station | 7.13 | 0.1 |
| | | | Medium Arias Intensity | Kocaeli, Turkey | 1155 | 289.69 | 60.43 | 1999 | Bursa Tofas | 7.51 | 0.5 |
| | | | High Arias Intensity | Manjil, Iran | 1634 | 302.64 | 75.58 | 1990 | Abhar | 7.37 | 1.9 |
| | | Stiff soil 400-760 m/s | Low Arias Intensity | Chalfant Valley | 557 | 467.62 | 50.92 | 1986 | Tinemaha Res. Free Field | 6.19 | 0.0 |
| | | | Medium Arias Intensity | Caldiran, Turkey | 1627 | 432.58 | 50.78 | 1976 | Maku | 7.21 | 0.1 |
| | | | High Arias Intensity | Big Bear | 928 | 564.11 | 63.92 | 1992 | Sage - Fire Station | 6.46 | 0.6 |
| | | Rock 760-1500 m/s | Low Arias Intensity | Chi-Chi, Taiwan | 2759 | 789.18 | 65.26 | 1999 | HWA002 | 6.2 | 0.0 |

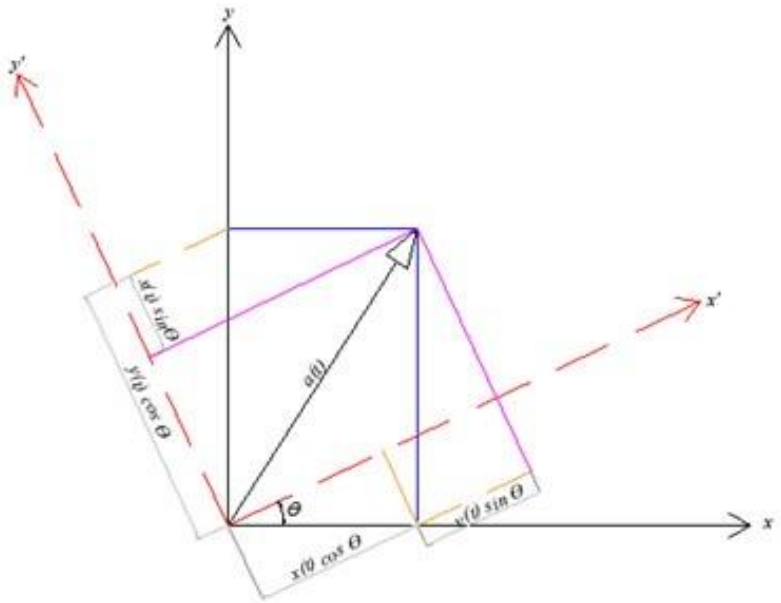


**Figure 2.** Orientation of the Axes with Respect to the Incident Angle.

## RESULTS AND DISCUSSION

In this study, the impact of the orientation of recorded earthquake data on a 10-story RC building is investigated. Figure 3 presents the comparison of base shear results of the oriented data with original data for normal, reverse, and strike-slip faults. As it is evident that the results from the rotated data reverse, and strike-slip earthquakes dominate the results of the original data. On the other hand, the base shear based on rotated data and those based on original data share the same trend. Focusing on the rotated earthquake data reveals a substantial increase in results for reverse

and strike-slip earthquakes compared to the unrotated earthquake data. This effect is evident in earthquake data like RSN 828 (reverse) and RSN 3968 (strike-slip), where the rotated data show a clear amplification.

Figure 4 depicts the roof displacement values calculated using rotated earthquake data, which often differ from those obtained from the original, unrotated data. This discrepancy is observed across most fault types. Some earthquakes with reverse or strike-slip fault mechanisms exhibit less pronounced differences between original and rotated data. In an earthquake with strike-slip faulting, the rotated RSN3968 earthquake data produced a roof displacement calculation three times greater than the displacement calculated from the original data. This highlights the potential for substantial variation in results depending on data orientation. Typically, earthquake data concerning reverse and normal fault mechanisms are mostly influenced by rotation. In contrast, results from earthquake data of strike fault mechanism show consistent outcomes between original and converted data.

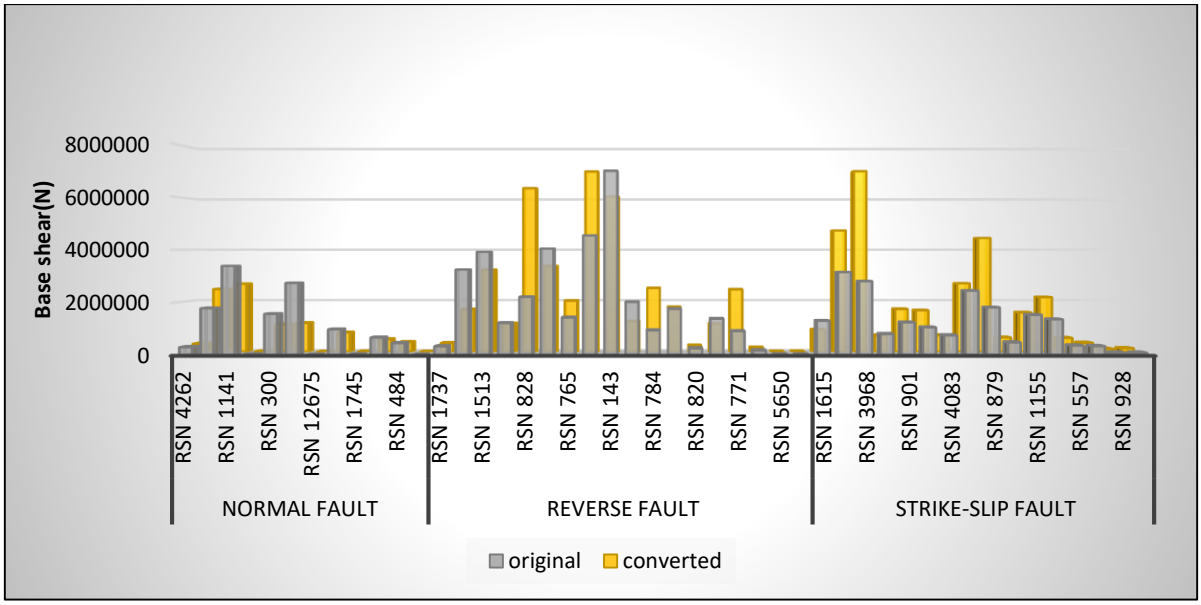


**Figure 3.** Comparison of Base Shear with Original Data and Rotated Data using both Horizontal Directions (Normal, Reverse, and Strike-slip Faults)

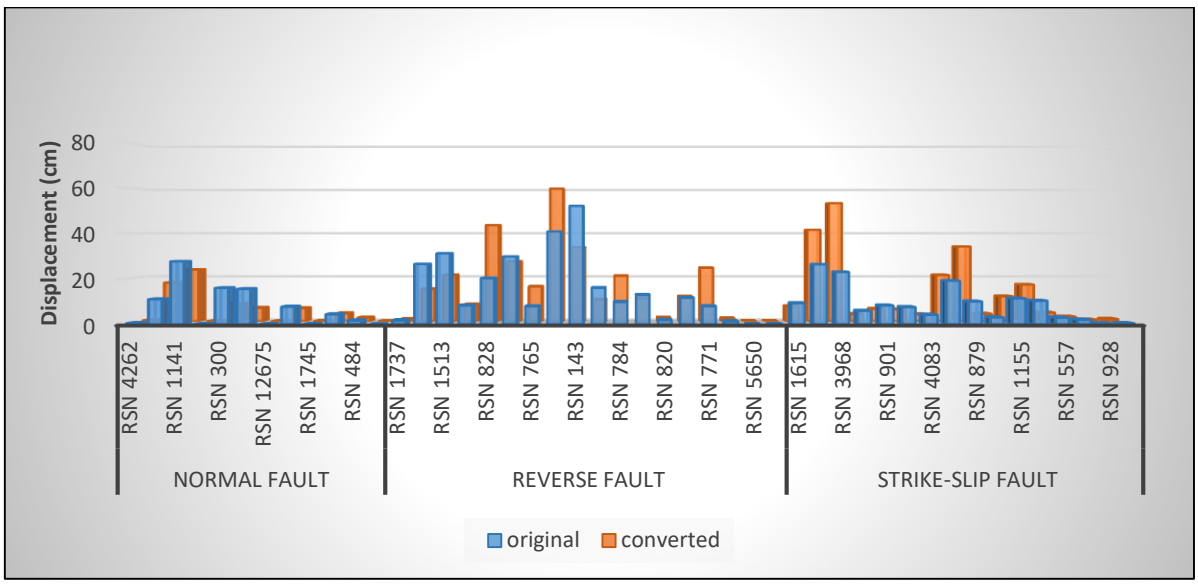


**Figure 4.** Comparison of Roof Displacement with Original Data and Rotated Data using both Horizontal Directions (Normal, Reverse, and Strike-slip Faults).

To better understand and interpret the results, the ratio between the roof displacement and base shear based on original data and rotated data is obtained for each station. As expected, both the ratio of roof displacement and the ratio of base shear are consistent with each other.

**Table 4.** The Ratio between Original and Rotated results for Roof Displacement and Base Shear.

| Fault Type | Near/Far Field | Soil Type | Arias Intensity | Record Sequence Number | Displacement | Base shear |
|---|---|---|---|---|---|---|
| | | | | | Original/ Converted | Original/ Converted |
| Normal Fault | Near Field | Soft soil 0-400 | Low Arias Intensity | RSN 4262 | 0.873 | 0.900 |
| | | | Medium Arias Intensity | RSN 564 | 0.627 | 0.722 |
| | | | High Arias Intensity | RSN 1141 | 1.178 | 1.268 |
| | | Stiff soil 400-760 | Low Arias Intensity | RSN 113 | 0.534 | 0.878 |
| | | | Medium Arias Intensity | RSN 300 | 1.987 | 1.437 |
| | | | High Arias Intensity | RSN 4480 | 2.539 | 2.396 |
| | | Rock 760-1500 | Low Arias Intensity | RSN 12675 | 0.846 | 0.693 |
| | Far Field | Soft soil 0-400 | High Arias Intensity | RSN 1127 | 1.294 | 1.276 |
| | | Stiff soil 400-760 | Low Arias Intensity | RSN 1745 | 1.081 | 1.126 |
| | | | Medium Arias Intensity | RSN 293 | 1.212 | 1.320 |
| | | | High Arias Intensity | RSN 484 | 1.009 | 1.155 |
| | | Rock 760-1500 | Low Arias Intensity | RSN 16678 | 1.452 | 1.638 |
| Reverse Fault | Near Field | Soft soil 0-400 | Low Arias Intensity | RSN 1737 | 1.783 | 0.937 |
| | | | Medium Arias Intensity | RSN 4210 | 1.805 | 1.936 |
| | | | High Arias Intensity | RSN 1513 | 1.481 | 1.217 |
| | | Stiff soil 400-760 | Low Arias Intensity | RSN 410 | 1.075 | 1.087 |
| | | | Medium Arias Intensity | RSN 828 | 0.464 | 0.345 |
| | | | High Arias Intensity | RSN 1507 | 1.094 | 1.201 |
| | | Rock 760-1500 | Low Arias Intensity | RSN 765 | 0.501 | 0.712 |
| | | | Medium Arias Intensity | RSN 3548 | 0.677 | 0.644 |
| | | | High Arias Intensity | RSN 143 | 1.546 | 1.152 |
| | Far Field | Soft soil 0-400 | Low Arias Intensity | RSN 510 | 1.629 | 1.684 |
| | | | Medium Arias Intensity | RSN 784 | 0.475 | 0.375 |
| | | | High Arias Intensity | RSN 578 | 1.247 | 0.997 |
| | | Stiff soil 400-760 | Low Arias Intensity | RSN 820 | 1.184 | 0.988 |
| | | | Medium Arias Intensity | RSN 14 | 1.033 | 1.252 |
| | | | High Arias Intensity | RSN 771 | 0.328 | 0.370 |
| | | Rock 760-1500 | Low Arias Intensity | RSN 2989 | 1.014 | 1.009 |
| | | | Medium Arias Intensity | RSN 5650 | 0.842 | 1.284 |
| | | | High Arias Intensity | RSN 5646 | 0.884 | 0.907 |
| Strike-Slip Fault | Near Field | Soft soil 0-400 | Low Arias Intensity | RSN 1615 | 1.356 | 1.492 |
| | | | Medium Arias Intensity | RSN 1605 | 0.634 | 0.662 |
| | | | High Arias Intensity | RSN 3968 | 0.429 | 0.397 |
| | | Stiff soil 400-760 | Low Arias Intensity | RSN 1618 | 1.790 | 1.224 |
| | | | Medium Arias Intensity | RSN 901 | 1.458 | 0.736 |
| | | | High Arias Intensity | RSN 1617 | 1.399 | 0.643 |
| | | Rock 760-1500 | Low Arias Intensity | RSN 4083 | 1.321 | 1.132 |
| | | | Medium Arias Intensity | RSN 1165 | 0.909 | 0.910 |
| | | | High Arias Intensity | RSN 879 | 0.295 | 0.407 |
| | Far Field | Soft soil 0-400 | Low Arias Intensity | RSN 1812 | 0.890 | 0.832 |
| | | | Medium Arias Intensity | RSN 1155 | 1.002 | 0.986 |
| | | | High Arias Intensity | RSN 1634 | 0.621 | 0.633 |
| | | Stiff soil 400-760 | Low Arias Intensity | RSN 557 | 0.735 | 0.642 |
| | | | Medium Arias Intensity | RSN 1627 | 0.976 | 0.922 |
| | | | High Arias Intensity | RSN 928 | 0.578 | 0.661 |
| | | Rock 760-1500 | Low Arias Intensity | RSN 2759 | 0.440 | 0.558 |

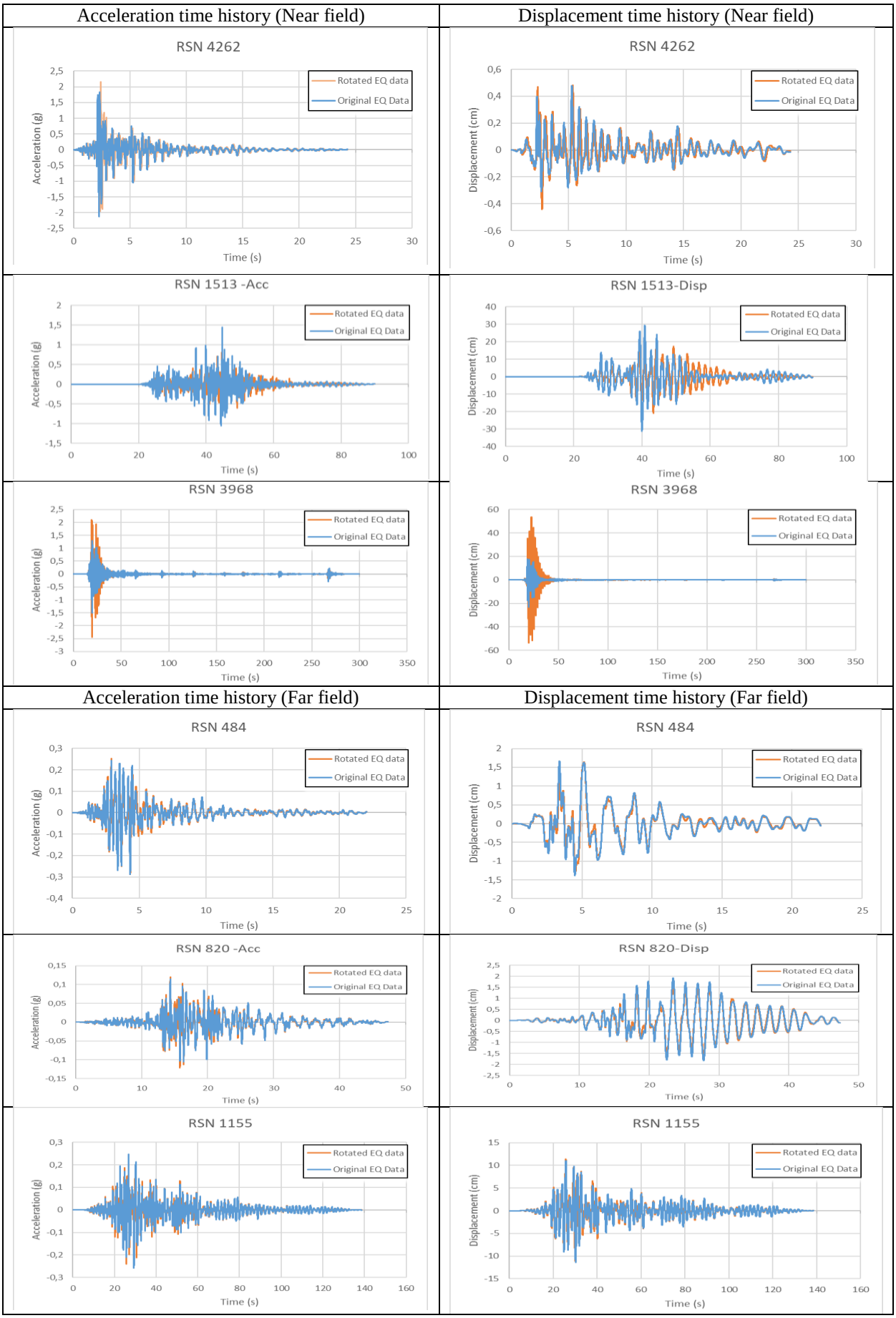


**Figure 5.** Comparison of Acceleration and Displacement Time Histories based on Original and Rotated Data for Near and Far Field

Figure 5 represents the acceleration and displacement time histories for the near and far fields. In the near-field acceleration and displacement data, there is a close agreement between the original and the rotated data of RSN4262 and RSN1513, unlike the acceleration and displacement of RSN3968 the rotated data overestimates the original data. There might be potential amplification effects. For the far-field in graphs of RSN1155, similar trends were observed for both data sets. Also, a distinct difference between rotated and original data, indicating a significant impact of rotation on displacement and acceleration behaviour for RSN484 and RSN820.

In Figure 5, in some cases like RSN3968, rotated data amplifies the original data. The rotated data from near-field earthquakes exhibits higher peak values indicating a potentially stronger shaking direction. However, far-field acceleration and displacement data have a similar trend for both original and rotated data.

Figure 6 represents the results for both original and rotated data align closely when examined across a range of Arias intensity values for normal, strike-slip, and reverse fault mechanisms. This suggests that data orientation might not significantly influence structural response based on arias intensity.

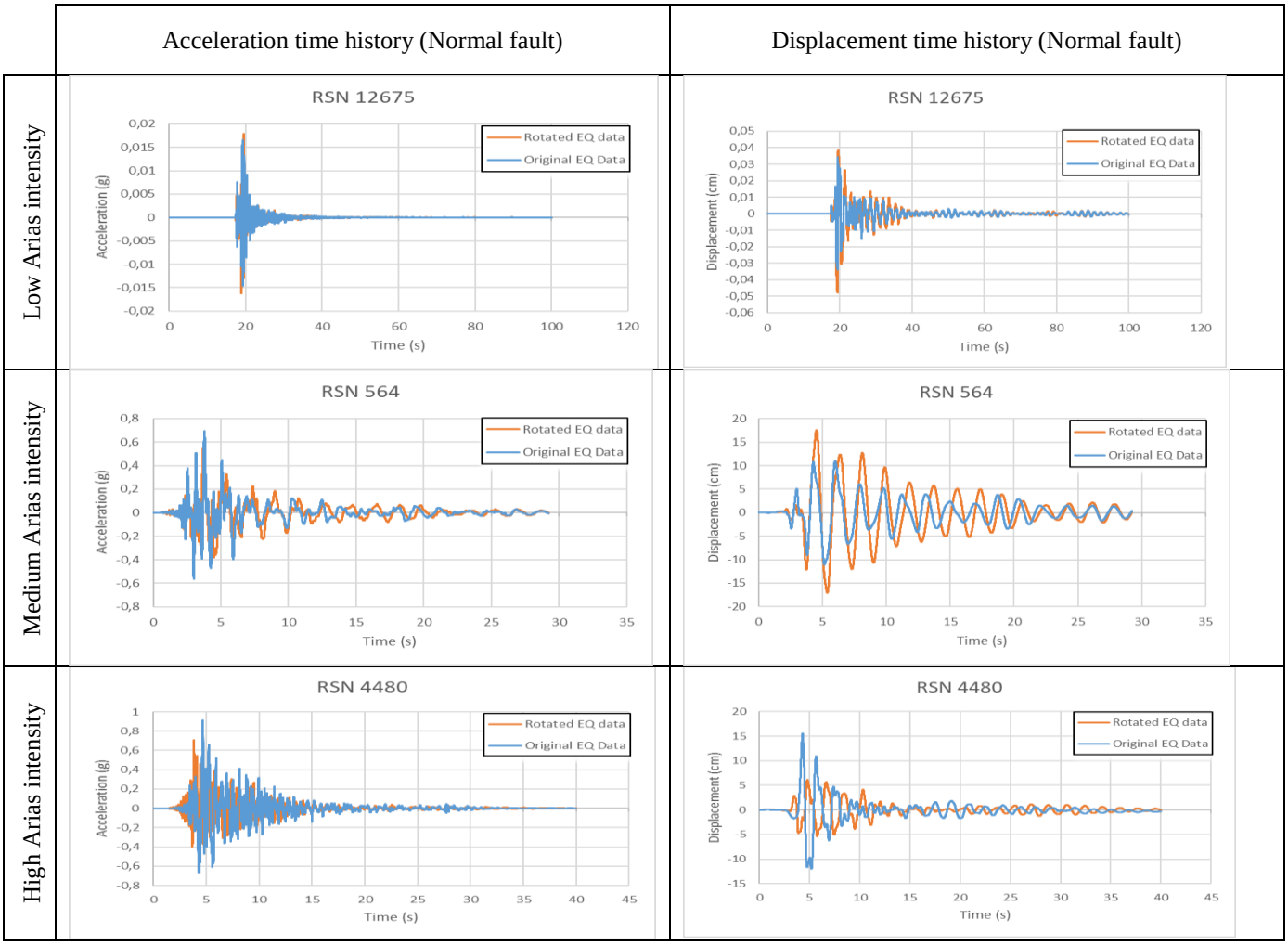


**Figure 6.** Comparison of Acceleration and Displacement Time Histories based on Original and Rotated Data Considering Low, Medium, and High Arias Intensity Values

In Figure 7, the acceleration and displacement time histories are represented concerning fault types. The rotated earthquake data tends to produce higher acceleration and displacement values compared to the original data (e.g. RSN113). The result in displacement from the rotated data of RSN113 reaches the maximum displacement at 1.8s. This proposes that considering data orientation is essential for a more conservative design approach. Unlikely, the results from the original data of RSN 300 show higher acceleration and displacement than those of the rotated data. This highlights the potential for specific earthquakes and fault mechanisms to exhibit unique behaviour that doesn't follow the general trend. This emphasises the importance of analysing both original and rotated data to avoid underestimating potential structural responses.

The rotated data of the record RSN828 reigns supreme in terms of acceleration. This means that analysing the earthquake with its direction shifted reveals the highest peak shaking compared to the original data. This observation underscores the potential for data orientation to sometimes amplify structural response in reverse fault scenarios. But it doesn't end there cause RSN765 flips the script, with the original data boasting a significantly higher acceleration than the rotated data. Despite this difference, both earthquakes share a remarkably similar path and shape in their acceleration time histories. This hints at a shared underlying characteristic, despite the varying peak values. Interestingly, both RSN828 and RSN765 reach their maximum displacement for the rotated data at almost the same time (3.5s). This synchronicity in peak displacement, despite differences in peak acceleration, adds another layer to understanding how reverse faults behave.


**Figure 7.** Comparison of Acceleration and Displacement Time Histories based on Original and Rotated Data Considering Normal, Reverse, and Strike-slip Faults

RSN879 brings us back to the familiar theme. Just like many other examples, the rotated data reigns supreme in terms of acceleration and displacement, surpassing the original version in the diagram. This reinforces the general trend that for strike-slip faults, considering data orientation might be crucial for a conservative design approach that

anticipates stronger shaking possibilities. On the other hand, RSN879, which captured the acceleration, revealed that the rotated earthquake data consistently surpassed the original data across the diagram but when we look at displacement RSN901, the original data prevails over the rotated.

Overall, for normal, reverse, and strike-slip faults, analysing rotated earthquake data generally leads to higher values compared to the original data.

The analysis compares the response of structures to near-field and far-field earthquakes by looking at their acceleration and displacement spectra in Figure 8. Notably, it highlights the contrasting behaviour between original and rotated earthquake data, particularly in the displacement spectra, where discrepancies tend to be more pronounced.

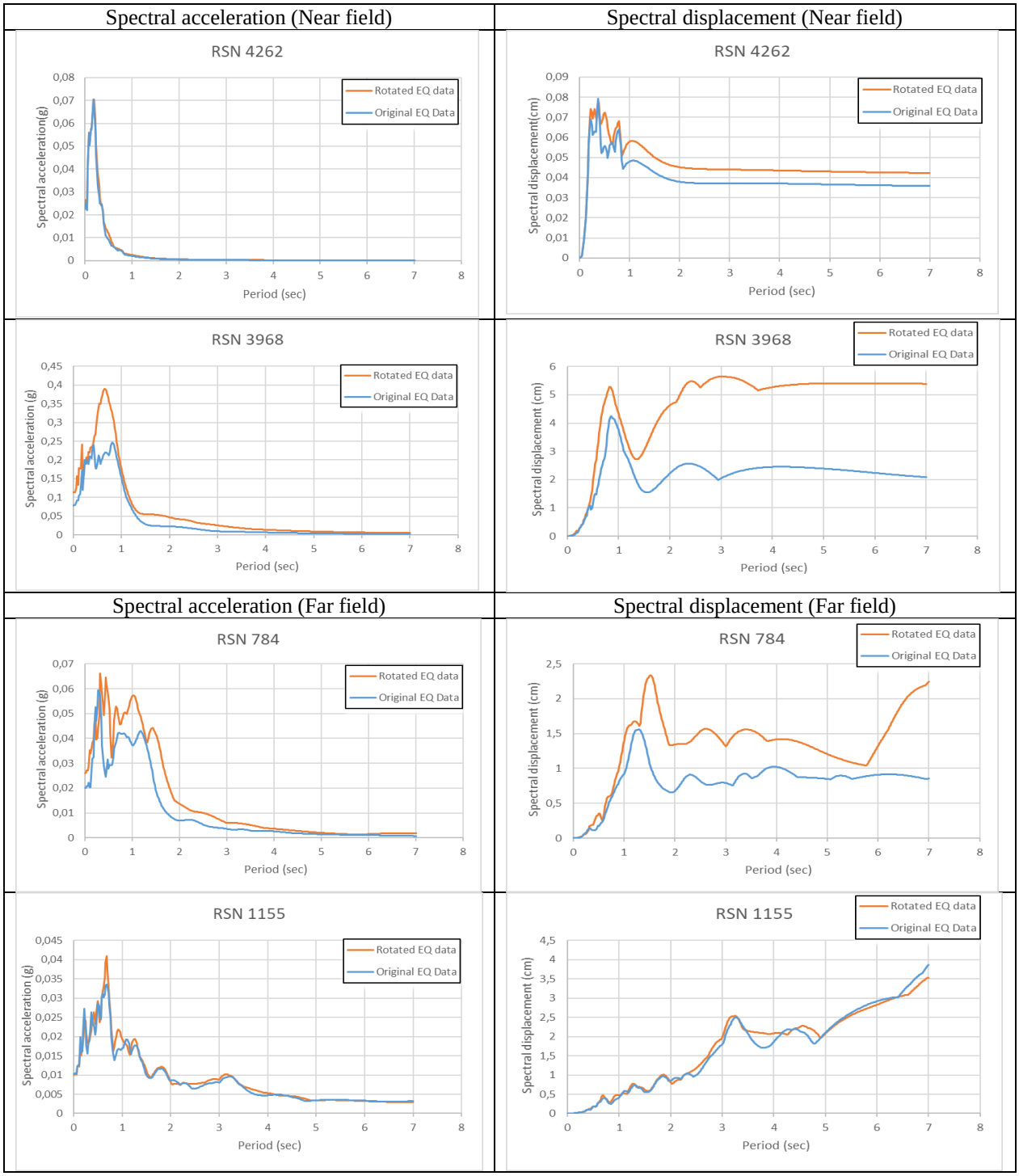


**Figure 8.** Comparison of Acceleration and Displacement Response Spectra based on Original and Rotated Data considering Near and Far field Effect

Figure 9 represents the comparison of acceleration and displacement response spectra based on original and rotated data. These spectra were generated for low, medium, and high Arias Intensity values ranging from 0 to 7 seconds. The rotated data generally covers the original data across all intensity levels, except for RSN484. This means that considering data orientation often leads to higher predicted values for both acceleration and displacement, suggesting a more conservative design approach might be necessary.

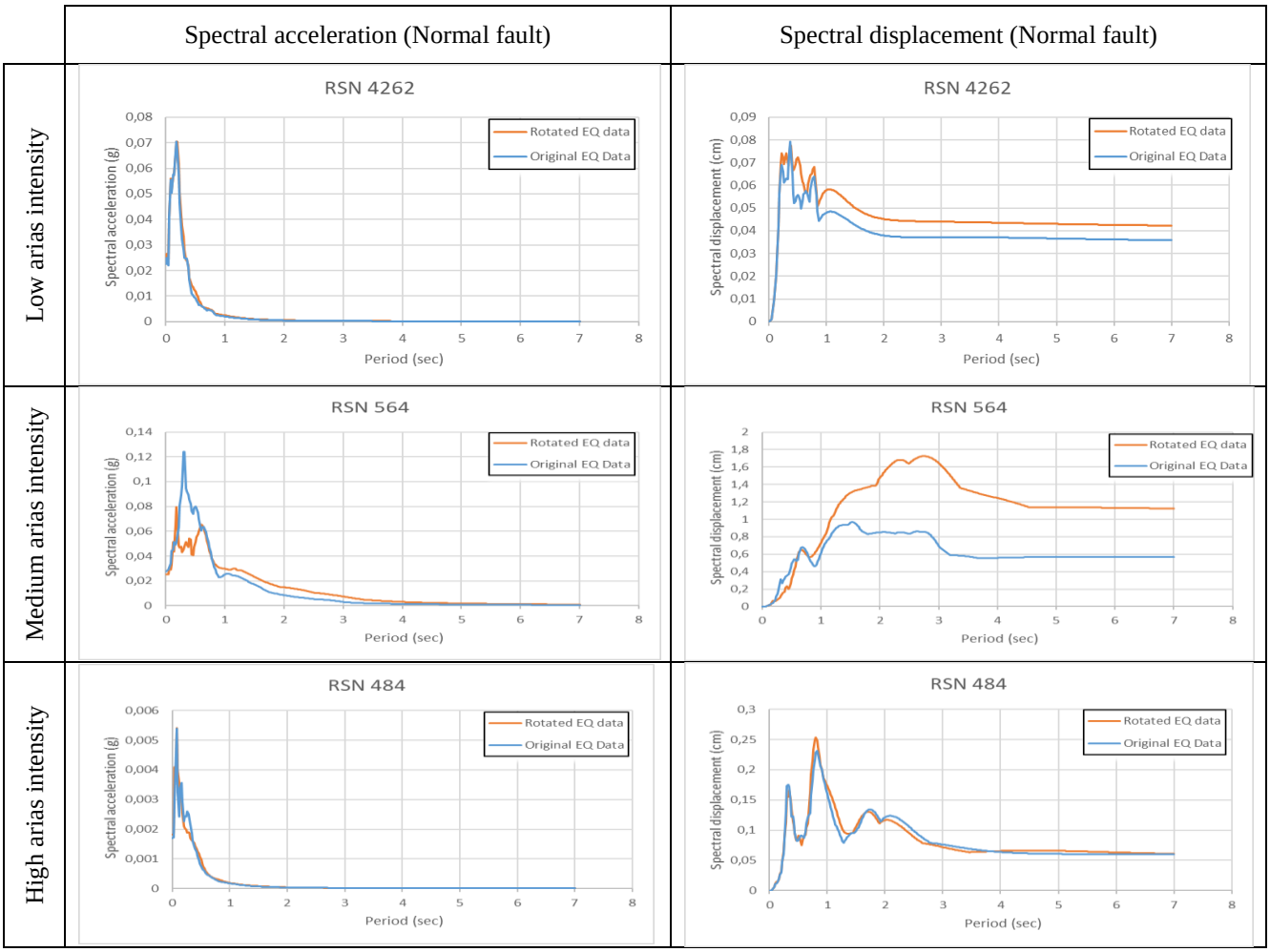


**Figure 9.** Comparison of Acceleration and Displacement Response Spectra based on Original and Rotated Data considering Low, Medium, and High Arias Intensity Values

The results based on the normal faults paint a similar picture in the response spectra for both the original and rotated data. Acceleration and displacement values largely agree, suggesting a good level of correspondence between how a building might react when the earthquake comes head-on or from a slightly different angle. This "harmony" can potentially simplify design considerations for structures facing normal fault mechanisms. The scene shifts with reverse faults because here, the original data often takes the reins in terms of acceleration and displacement response. Analysing the raw, unadjusted data seems to reveal the strongest potential shaking for these earthquakes. This finding highlights the importance of not solely relying on rotated data for reverse fault scenarios, as it might underestimate the structural response, but when it comes to strike-slip faults, the plot thickens. Here, a stark difference emerges between the original and rotated data. The gap between the curves widens considerably, especially for displacement. This divergence underlines the significant impact of data orientation on how structures might experience shaking from these side-sliding earthquakes. Simply analysing the original data could potentially miss the full picture of potential building movements.

Figure 10 depicts the comparison of acceleration and displacement time histories based on original and rotated data considering normal, reverse, and strike-slip faults. This analysis delves into the earthquake directionality, exploring how it influences the movement of structures through acceleration and displacement time histories, as well as response spectra (0-7 seconds). For normal faults, the original and rotated data often overlap closely, suggesting that the direction of the earthquake doesn't significantly alter the building's response. However, RSN300 stands out: a

huge difference emerges between the two datasets in both acceleration and displacement, highlighting the potential for individual earthquakes to deviate from the general trend. In reverse faults, here, the rotated data generally reigns supreme, surpassing the original in both acceleration and displacement, as exemplified by RSN1737 and RSN14. This suggests that considering data orientation is crucial for these faults, as it can reveal potentially stronger shaking scenarios. For strike-slip faults present a captivating contrast, in the displacement response spectra, RSN557 shows the rotated data soaring above the original with a substantial gap. This reinforces the importance of data orientation for strike-slip faults, as ignoring rotated data might underestimate potential building displacements. However, in RSN1627, the original data outperforms the rotated, reminding us that individual earthquakes can defy even the most established trends.

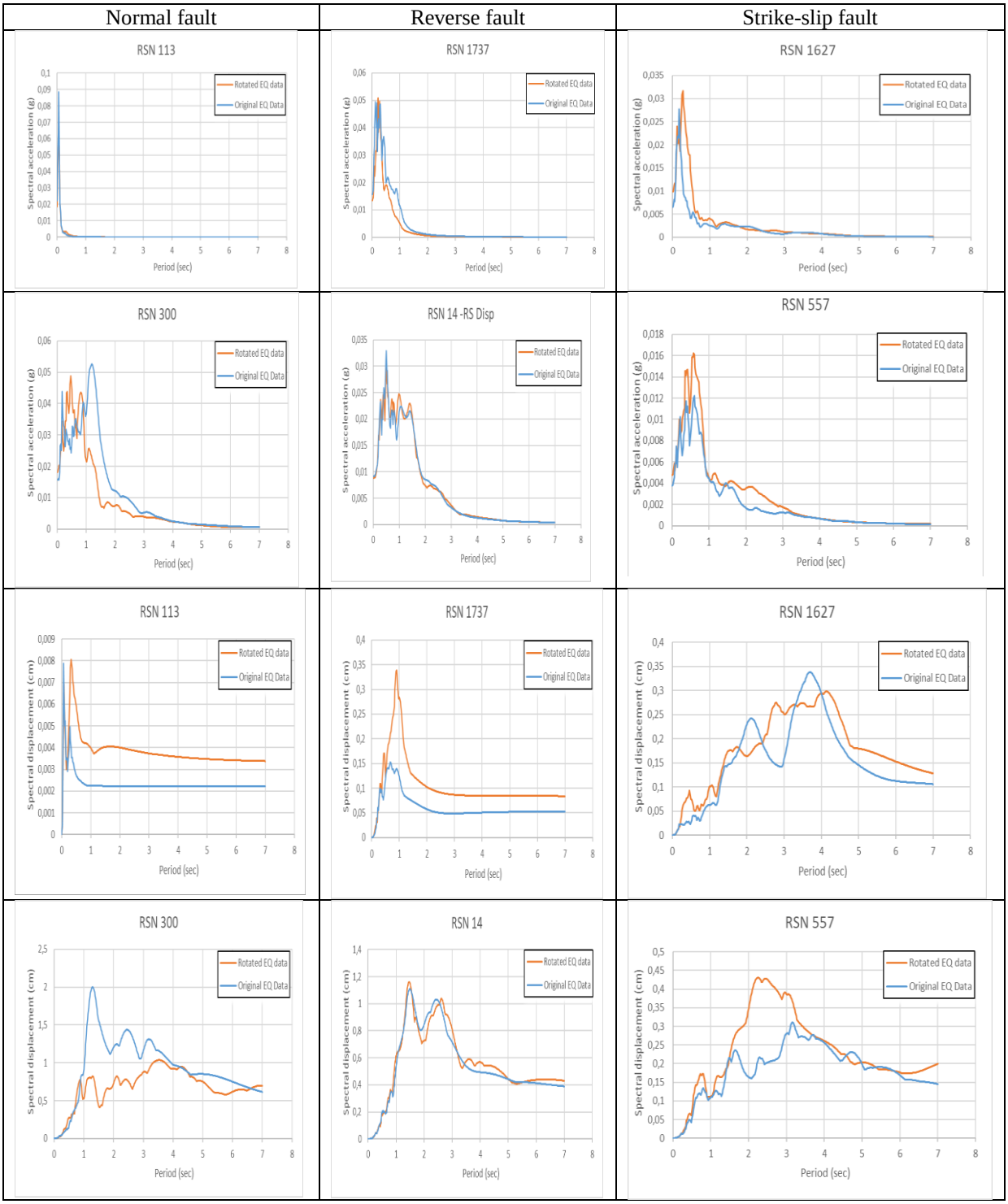


**Figure 10.** Comparison of Acceleration and Displacement Response Spectra based on Original and Rotated Data considering Normal, Reverse, and Strike-slip Faults

In this study, the impact of the soil type was also examined, yet no significant difference was detected.

## CONCLUSION

Identifying the critical earthquake data that poses the greatest threat to a structure can be a complex puzzle. Past research has highlighted the variability of earthquake effects based on their direction, measured by the incident angle. Recognizing this, researchers have developed the concept of earthquake ground motion critical angles, which identify the angle that produces the maximum response in a structure.

This study delves deeper into this area by examining the specific impact of incident angle on a 10-story reinforced concrete (RC) building. The earthquake data is rotated around the building, simulating different shaking directions, and analyse the resulting changes in response, particularly focusing on the maximum acceleration experienced by the structure.

The foremost critical discoveries of this work can be summarized as

Analysing acceleration and displacement time histories across diverse fault types (strike-slip, normal, and reverse) revealed a consistent trend: rotated earthquake data generally yielded higher peak values than the original data. This suggests that both fault type and individual fault characteristics significantly influence structural response, highlighting the importance of considering data orientation in earthquake engineering.

Across all fault types (normal, reverse, and strike-slip), the base shear and roof displacement results consistently show that rotated earthquake data overestimates the values obtained from the original data. This trend is readily apparent in visualized time histories or overlay plots of these responses, where the rotated curves consistently lie above the original curves. The distance (near-/and far-field) of the earthquakes affects the results of acceleration and displacement time histories. As expected, the results from near-field data outweigh the results from far-field data.

The acceleration and displacement response spectra are studied for near and far-field scenarios, comparing original and rotated data. Notably, rotation amplified the long-period components, meaning both acceleration and displacement values in this range were noticeably higher compared to the original data. This suggests data orientation plays a critical role in understanding how structures might respond to long-period earthquake motions.

The examination of normal, reverse, strike-slip faults and arias intensity for acceleration and displacement response spectra exposes that some of the results of the rotated earthquake data exceed the results of the original data to hold out the maximum value. However, generally, there is no difference in terms of Arias intensity.

At the end of the study, it is concluded that a detailed examination of the direction of earthquake records leads to a proper situation for sensitive structures because finding the exact maximum point after calculation of different incident angles of θ will help the studies on the earthquake and civil engineering to ensure that structures can safely withstand against earthquakes.

## REFERENCES

Altunışık, A.C., & Kalkan, E. (2017). Earthquake incidence angle influence on seismic performance of reinforced concrete buildings. S*igma Journal of Engineering and Natural Sciences*, 35, 609-631.

Athanatopoulou, A.M. (2005). Critical orientation of three correlated seismic components. *Engineering Structures*, 27, 301-312. https://doi.org/10.1016/j.engstruct.2004.10.011.

Bugueño, I., Carvallo, J., & Vielma, J.C. (2021). Influence of Directionality on the Seismic Response of Typical

RC Buildings. Academic Editor: Maria Favvata, 12, 1534. https://doi.org/10.3390/app12031534.

Cantagallo, C., Terrenzi, M., Camata, G., & Spacone, E. (2024). Historical Evolution of the Impact of Seismic Incident Angles on the Safety Assessment of Various Building Construction Typologies. *Department of Engineering and Geology*, 14, 1490. https://doi.org/10.3390/buildings14061490.

Ghazizadeh, S.A., Grant, D., & Rossetto, T. (2013). Orientation dependence of ground motion and structural response of reinforced concrete space frames, Vienna Congress on Recent Advances in Earthquake Engineering and Structural Dynamics, Vienna, 71, (pp. 28-30).

Hong, H.P., Pozos-Estrada, A., & Gomez, R. (2009). Orientation effect on ground motion measurement for Mexican subduction earthquakes. *Earthquake Engineering and Engineering Vibration*, 8, 1-16. https://doi.org/10.1007/s11803-009-8155-z.

Huang, Y.N., Whittaker, A.S., & Luco, N. (2009). Orientation of maximum spectral demand in the near-fault region. *Earthquake Spectra*, 25, 707-717. https://doi.org/10.1193/1.3158997.

Kostinakis, K. G., Manoukas, G. E., & Athanatopoulou, A. M. (2018). Influence of seismic incident angle on response of symmetric in plan buildings. *KSCE Journal of Civil Engineering*, 22, 725-735. https://doi.org/10.1007/s12205-017-1279-1

Kostinakis, K.G., Athanatopoulou, A.M., & Avramidis, I.E. (2012). Orientation effects of horizontal seismic components on longitudinal reinforcement in R/C frame elements. *Natural Hazards and Earth System Sciences*, 12, 1-10. https://doi.org/10.5194/nhess-12-1-2012, 2012.

Lee, J. (2014). Directionality of strong ground motion durations, In Tenth US National Conference on Earthquake Engineering, Anchorage, (pp. 21-25).

Pinzon, L.A., Diaz, S.A., Pujades, L.G., & Vargas, Y.F. (2021). An efficient method for considering the directionality effect of earthquakes on structures, *Journal of Earthquake Engineering*, 25, 1679-1708. https://doi.org/10.1080/13632469.2019.1597783.

Ruiz-García, J., & Negrete-Manriquez, J.C. (2011). Evaluation of drift demands in existing steel frames under as-recorded far-field and near-fault mainshock–aftershock seismic sequences, *Engineering Structures*, 33, 621-634. https://doi.org/10.1016/j.engstruct.2010.11.021.

Sun, M., Fan, F., Sun, B., & Zhi, X. (2016). Study on the effect of ground motion direction on the response of engineering structure. *Earthquake Engineering and Engineering Vibration*, 15, 649-656. https://doi.org/10.1007/s11803-016-0355-8.

TBEC. (2018). Turkish Building Earthquake Code. Disaster and Emergency Management Agency (AFAD).